CURRENT COLLECTION BY A SEGMENTED LANGMUIR PROBE IN THE IONOSPHERIC PLASMA

E. Séran
CETP, 4 Avenue de Neptune
94100 Saint-Maur, France

J.-J. Berthelier
CETP, France

J.-P. Lebreton
ESA/ESTEC, The Netherlands

Abstract

The segmented Langmuir probe (SLP) has been recently proposed by one of the authors (Lebreton, 2002) as an instrument for the newly prepared ionospheric mission DEMETER to determine the plasma bulk velocity in addition to the electron density and the temperature that are routinely deduced from the Langmuir probe data. The basic idea of the SLP concept is to measure the current distribution on the probe surface by means of the individual segments and then to use the current anisotropy to estimate the amplitude and the direction of the plasma bulk speed in the probe frame. With the aim to evaluate the performances of such a probe we have developed a numerical particle in cell (PIC) model which provides a tool to calculate the current collection by spherical probe and its segments. This model is based on the simultaneous determination of the charge densities in the near-probe sheath and on the surface of the probe which are then used to compute the potential distribution in the sheath region. This scheme is well adapted to the SLP problem and has an advantage with respect to other classical probe models, i.e. it provides a natural control of the charge neutrality inside of simulation box. Comparison of the results of our model with the exact solution given by Laframboise for the spherical probe in thermal non-flowing plasma demonstrates an excellent agreement. Here we present the results for the bulk thermal plasma in the case when Debye length and sphere radius have approximately the same values, i.e. few cm. These conditions are expected to be observed in the ionosphere at the altitude of ~700 km and therefore our model may be directly applied for the interpretation of the current measurements on the board the DEMETER satellite.

Introduction

Since the advent of the space era, the Langmuir probe is proven to be very efficient tool to study space plasmas by measuring two fundamental parameters, i.e. the electron density and the temperature, which are the key parameters that control the production and dynamics of the ionised environments of the Earth and planets. This instrument is one of the most used in the space missions because of its relative simplicity, light weight, easiness of operation and data reduction. Numerous papers have been published in the course of the last decades on theoretical studies and experimental validation of the operation of Langmuir probes in laboratory, ionospheric and magnetospheric plasmas. More generally, the problem of the spacecraft interaction with the ambient plasma has also attracted much attention (Al'pert, 1974 and references therein) because the charging processes and the electrical equilibrium of spacecraft are vitally important for the onboard observations. If analytical models have been used in initial studies (Laframboise, 1966; Sanmartin, 1970; Laframboise and Sonmor, 1993),

a number of numerical models have been developed since then (see, for example, Jolivet and Roussel, 2001; Roussel and Berthelier, 2003) because they are the only way to cope with complex geometries and variety of physical processes that must be taken into account.

The objective of our work is to study the operation and performances of a new concept of the segmented Langmuir probe in order to take benefit of the above mentioned advantages of conventional Langmuir probes while extending their capabilities by accessing to plasma bulk velocity. Since the first flight of the SLP will be onboard the DEMETER CNES micro-satellite we have concentrated our study on plasma conditions typical for the ionosphere at the altitude of ~700 km, where the Debye length and probe radius have approximately the same values, i.e. few cm, thermal ion velocity, plasma bulk velocity in the probe frame and thermal electron speed are related as $V_{Ti} \leq V_0 << V_{Te}$. In such conditions the plasma flow mainly modifies the ion current, the collection and the distribution of which on the probe surface is controlled by the ratio of the bulk velocity to the thermal ion velocity and also by the potential that applied to the probe. In the present configuration the SLP contains 7 circular caps which are electrically insulated from the rest probe surface and therefore may be considered as individual collectors, which allow to measure the angular anisotropy of the collected current. With the aim to simulate the current collection by the SLP in the flowing ionospheric plasma we have developed an electrostatic model of the particle in cell (PIC) type. Our model is based on the method which was proposed by one of the authors (Kolesnikova, 1997; Béghin and Kolesnikova, 1998) to determine the frequency response of electrostatic HF probes in plasmas. This method differs from the commonly adopted numerical scheme to solve the Poisson equation, i.e. the electrical potential is directly evaluated from the ensemble of charges in the near-probe sheath and on the probe surface, and has the advantage, i.e. it allows a natural control of the total charge neutrality of the system probe-sheath.

In the chapter 2 we describe the method and illustrate it for the case of spherical probe, in chapter 3 present numerical solution for non-flowing thermal plasma and compare it with exact solution of Laframboise, in the chapter 4 give results for the bulk thermal plasma and examine a possibility to use segmented probe for the flow diagnostics in the ionospheric conditions. Future development of our model is discussed in the conclusion.

Description of the model

We first wish to review very briefly the main principles of our model. The SLP is located in a centre of the simulation box divided into elementary cells by a 3D mesh. Ions and electrons are injected from the sides of the box and subsequently move under the action of electric field in the near-probe sheath (and possibly of a static magnetic field). After each computation step, the charge density deposited in each cell by electrons and ions is computed. Similarly, the surface charge density on each element of the probe surface is calculated to satisfy the condition that all contributing charges, i.e. in the sheath and on the probe surface, sum up to create the desired polarization potential on the probe surface. The newly computed space and surface charges are then used to iterate the electric field for the next computation step. The particles that hit the probe surface are lost from the system and contribute to the collected current. After a number of computation steps, the system converges towards a stationary state which provides the solution we are looking for. In the following paragraphs we expose in more details the main features and parameters of our model.

Size of the simulation box

Conditions of the charge neutrality and the density continuity at the box boundary presume that the boundary has to be placed at least outside of the sheath region, dimensions of each are determined by a variety of parameters, i.e. size and form of obstacle, applied potential (in the case of the conducting surface), ratio of the bulk and thermal velocities, characteristic plasma lengths, magnitude of the magnetic field, etc. Basic ideas of the cavity size around the charged obstacle in plasma may be borrowed from the estimations of its size in the case of non-charged body. For example, in a motionless plasma the variation of the density n as a function of distance r from the centre of the sphere can be written as

$$n/n_0 = 0.5\left(1+\sqrt{1-[r_s/r]^2}\right), \qquad (1)$$

where n_0 is the undisturbed density and r_s is the probe radius. By this way, the density differs by 2% from the undisturbed value at a distance ~4 r_s. The corresponding formula for the density variation in the wake behind a probe in a flowing thermal plasma is

$$n/n_0 = 0.5\left(1-\Phi(\chi)+\cos\theta\exp(-\chi^2\sin^2\theta)(1+\Phi(\chi\cos\theta))\right), \qquad (2)$$

where $\chi = V_0/V_T$ is the ratio between the bulk and thermal velocity, $\theta = arctg(r_s/r)$ and Φ is the error function. Therefore the disturbed region in the wake extends till ~9 r_s for χ=1 and ~28 r_s for χ=4 . Polarised probe totally modifies the structure and the size of the sheath region. According to Laframboise (1966) the disturbed region around a spherical probe of the radius $1\lambda_D$ and of the potential 25 kT/e increases to ~13 r_s in the case of non flowing plasma, here λ_D is the Debye length, T is the temperature which is supposed to be the same for electrons and ions, k is the Boltzman constant and e is the absolute value of the elementary charge.

The correct choice of the simulation box size might be proven numerically by looking at the variation of the collected currents for the different box sizes with the aim to ensure the inaccuracy on the currents less than 2%.

Cell size and time step

Size of the integration cell is determined by the minimal characteristic length of the system plasma-obstacle. In particular case of the observations in the ionosphere at the altitude of ~700 km the Debye length, the typical linear dimension of electrostatic probes and the Larmor radius are related as $\lambda_D \le r_s < r_L$. Therefore the characteristic cell size in such conditions is chosen to be equal $1\lambda_D$. In the non-magnetised plasma there exist two types of the particles motion, i.e. thermal and bulk. Thermal speed of the electrons is much larger than that of the ions, the last may have the same order of magnitude as the bulk velocity of plasma with respect to the probe in the conditions of the ionospheric satellite observations. Thermal electrons (hereafter we define the thermal velocity as $V_T = \sqrt{2kT/m}$, m is the mass of a particle) pass the distance of $1\lambda_D$ during the time $\omega_{pe}^{-1}/\sqrt{2}$ (here ω_{pe} is the angular electron

plasma frequency). To avoid the fluctuations of the density inside of the simulation box the characteristic time has to be small enough to integrate even minor energetic population, such as suprathermal electrons with the speed of $2V_T$, which consist of ~2% of the total population (assuming the last to be Maxwellien with $T = 0.2$eV). Taking into account these considerations the characteristic time for the electrons is chosen to be $0.25\omega_{pe}^{-1}$. However this time is extremely small for the ions which have the thermal speed in $\sqrt{m_i/m_e}$ times less than that of the electrons (hereafter we assume that all populations have the same temperature). Using the fact that we are interesting in a stationary solution, the characteristic time for each species is chosen by analogy with the considerations which were undertaken for the electrons and is defined to be equal $0.25\omega_{pe}^{-1}\gamma$, here $\gamma=\sqrt{m_i/m_e}/(1+V_0/V_{Ti})$. Similar techniques of the "numerical time step" was used by Jolivet and Roussel (2001) and Roussel and Berthelier (2003). Total time of the integration is the time when the computed parameters reach a stationary solution and the total charge of the system sheath-probe attains zero. Naturally, this time has to be superior the particle travel time through the simulation box.

To illustrate the above discussion we present in the Fig. 1 time variation of (a) the total current collected by spherical probe and (b) the total space and surface charges, which are computed for the case of the negatively polarised probe with $\varphi=-20\ kT/e$ in the thermal bulk plasma with $\lambda_D=2$cm, $T = 0.2$eV. Upper, middle and lower curves in the Fig. 1a correspond to the H^+ plasma with $V_0=V_{Tp}$, $V_0=2V_{Tp}$ and to the O^+ plasma with $V_0=4V_{TO}$, respectively. Blue lines represent calculated values of the ion current and red lines stand for their averages over a period $5\omega_{pe}^{-1}\gamma$. In all presented cases the computed currents are converged to their limit values at the end of the integration time. Correctness of the obtained solution is ensured by the charge neutrality of the system sheath-probe. Time variations of the total space (red line) and surface (blue line) charges are shown in the Fig. 1b for the case $V_0=V_{Tp}$. Charges are normalised by the surface charge in the vacuum, i.e. $4\pi\varepsilon_0 r_s\varphi$. At the end of the integration time the space and surface charges have opposite signs and converge to the same absolute value.

Particles injection

To reproduce the conditions of the non-disturbed plasma at the boundary of the simulation box 5 rules have to be fulfilled, i.e.

- velocity distribution has to be that in the infinity;
- space distribution has to be uniform;
- plasma has to be neutral;
- potential has to be zero (in absence of external electric field);
- number of macro-particles has to be sufficiently high to provide a good statistics.

In our model we generate the macro-particles with the Maxwellien velocity distribution which are uniformly distributed in the pre-box region of the width $\lambda_D/\sqrt{2}$ on each side of the

simulation box. The number of the generated macro-particles depends on the box volume and is chosen to provide ~180 particles of each species per cell at the box boundary. This number produces the dispersion of the collected current of ~5% from the average value (see Fig. 1a). Injection of the different plasma species is controlled by the imposing the potential value on the boundary of the simulation box to be equal 0. In the case of non-isotrope plasma (for example, flowing or magnetised) the condition of the "free boundary" (when the potential on the boundary is not fixed, but calculated at the same manner as in the internal points), might lead to the accumulation of the charge (positive or negative) inside of the simulation box and therefore might produce a violation of the total charge neutrality. An example of the potential distribution along the probe axis parallel to the vector of the bulk velocity in the H^+ plasma with $V_0 = V_{Tp}$ is shown in the Fig. 2. Plasma parameters and probe potential are the same as in the Fig. 1.

Surface and space charges

After each time step the charges deposited by ions and electrons in the cells are determined by a classical method. Each macro-particle is considered as a cube of dimension λ_D (this length corresponds to the undisturbed plasma) with a uniformly distributed charge inside of it. The macro-particle gives to each of the 8 adjacent cells a contribution equal to the common volume of this cube with the cell itself. The potential at the centre of any element k (either a cell in the volume surrounding the probe or a surface element of the probe) can be expressed as the sum of the individual contributions due (i) to the surface charges on the elements of the probe surface $i \neq k$, (ii) to the volume charges in the cells $j \neq k$, and (iii) to the charges of the element k itself, i.e.

$$\varphi_k = \sum_{i \neq k} \frac{q_{si}}{4\pi\varepsilon_0 r_{ik}} + \sum_{j \neq k} \frac{q_{vj}}{4\pi\varepsilon_0 r_{jk}} + \frac{q_k}{4\pi\varepsilon_0}\phi_{kk} \quad , \qquad (3)$$

here charge q of any element is supposed to be located at the centre of mass of the element, r_{lm} is the distance between the centres of the elements l and m and s_k (v_k) is the surface (volume) of element. The last term expresses the contribution of the charge of the element k itself which may be written (see Kolesnikova, 1997) as $\phi_{kk} = \frac{1}{s_k}\iint_{s_k} \frac{ds}{\rho_k}$ for surface element and $\phi_{kk} = \frac{1}{v_k}\iiint_{v_k} \frac{dv}{\rho_k}$ for space element, here ρ_k is the distance between the centre of mass and another point inside of the element. Once the volume charges in the cells are determined the surface charges on the sphere are computed by using equation (3) for each surface element k to express that the potential on the surface is equal to the desired value φ. This comes down to solving a linear system to get the surface charges. The complete set of volume and surface charges is then used to compute the electric field which will control the particles motion during the next time step.

The sphere is represented by an assembly of pentagons and hexagons each of them might be cut into the smaller elements. For the simple case of a sphere in vacuum, the approximation of the sphere by an assembly of planar elements results in an underestimate of the total charge by about 5% compared to the true value $4\pi\varepsilon_0 r_s$. The same ratio between true and computed charges must also globally hold in the presence of a sheath since this is only a

geometrical effect. We can take this into account by multiplying the contributions of the surface charges by 1.05 in expression (3).

Particles hitting the surface of the probe are lost from the system, but give a contribution to the current, j, which is collected by a surface element. This current is calculated as $j = -\sum_i e_i N_i / \tau$, where e_i is the species charge (negative for electrons and positive for ions) and N_i is the number of particles of i-species collected by a surface element during the time step τ. Particles hitting the side of the box are lost. Photoelectrons that are emitted by the probe under solar UV radiation have not been taken into account in this version of the code.

Probe Response in Non-Flowing Thermal Plasma

In order to validate our model we have compared the results with the exact solution provided by Laframboise (1966) for an attractive probe in a non-flowing thermal plasma. This comparison was made for a probe with radius r_s = 2 cm, similar to the SLP which will be flown on DEMETER, and for plasma conditions close to those anticipated along the orbit, i.e. density ~$2.8 \cdot 10^4$ cm^{-3}, equal ion and electron temperatures $T_e = T_p = 0.2$eV, that correspond to $\lambda_D = 2$cm and $r_s/\lambda_D = 1$. Displayed in Fig. 3 are the theoretical values of the current of attracted particles for several potentials shown by blue dots and our model results represented by red dots. Potential is normalized by the plasma temperature and collected current by its value at $0V$ which is $j_0 = 2\sqrt{\pi} e r_s^2 n V_T$. The current-voltage characteristics, shown as solid lines, has been fitted by the analytical law

$$j/j_0 \approx \alpha \left[1 - \frac{e_i \varphi}{kT}\right]^{\kappa}, \; e_i \varphi \le 0, \tag{4a}$$

with $\alpha = 1$, $\kappa = 0.95$.

Fig. 4 displays the model currents for protons (blue dots) and for electron (red dots) in the probe potential range from $-6\,kT/e$ to $6\,kT/e$. The total current, sum of the ion and electron currents, is shown by solid line for the H^+ plasma and by dashed line for the O^+ plasma. Currents for repelling particles are fitted by the analytical law

$$j/j_0 \approx \alpha b^{-\frac{e_i \varphi}{kT}}, \; e_i \varphi \ge 0, \tag{4b}$$

with $\alpha = 1$, $b = 2.25$. Floating potentials are $\approx -3kT/e$ for H^+ plasma and $-4.5kT/e$ for O^+.

Presented in Fig. 5 are (a) the density distribution for attracted (blue) and repelling (red) particles, (b) the potential profile in the sheath. Analytical solution is shown by solid line and model results by dots. The nearly perfect agreement between theoretical and model results, with maximum differences less than ~ 3%, convincingly proves the validity and good accuracy of our code.

Probe Response in Bulk Thermal Plasma

Bulk velocity of plasma with respect to the probe produces an asymmetry of the charge distribution in the sheath region and therefore modifies the current collection and leads to an asymmetry of the current distribution on the probe surface. In case of on-board satellite observations in the ionosphere the bulk velocity mainly arises from the satellite movement (~7 km s^{-1}), proper plasma velocity might consist up to ~10% of the satellite speed. Most adapted instrument to measure the ion flows in such conditions is the retarding analyser (see, for example, Hanson, 1970; Séran, 2003). Segmented spherical probe was proposed as an alternative technique to resolve the bulk velocity. Here we examine this possibility, by analysing (i) current which is collected by entire probe and (ii) angular distribution of the currents which are measured by individual segments placed on the probe surface.

(i) In the conditions of ionospheric observations bulk speed of plasma with respect to the probe is much less than electron thermal velocity, but has the same order of magnitude as ion thermal speed. Therefore plasma flow will mainly modify the ion branch of the collected current. In Fig. 6 collected currents versus potential which is applied to the probe are presented for the cases of H^+ plasma in the conditions V_0=0 (black), V_0=V_{Tp} (blue), V_0=2V_{Tp} (green) and of O^+ plasma with V_0= 4V_{To} (red). Dots are used to indicate computed values, lines stand for their fittings by the law (4). Plasma characteristics are chosen the same as in the Fig. 1. The presented solutions demonstrate that decrease of the ion current might be caused by two effects, i.e. increase of the bulk velocity and presence of the heavy ions. Therefore the proper plasma speed (which consists only some percents of the total bulk speed) may be resolved from the Langmuir probe measurements only if the exact ion composition is known. An additional complexity in the interpretation of the negatively polarised probe measurements arises from the photoelectron emission from the probe surface. Under the action of the sun ultra-violate radiation the photoelectron current may attain amplitude of the ion current in the oxygen-dominated plasma. In such circumstances the possibility of the velocity determination from the probe measurements in the dayside ionosphere commences to be doubtable.

(ii) Currents, which are collected by the individual segments placed on the probe surface, maintain information about plasma anisotropy related to the flow. Under the action of electric field in the sheath region, the ions will be speed up in the lobe part and slow down in the wake. En consequence, the lobe part of the probe sheath will have luck of the positive charge and the wake will be overloaded with ions. The distribution of the ions in the sheath is controlled by the probe potential, or more precisely by the ratio of the ion energy to the attractive energy which is created by the polarised probe. Because we are interesting in the ion branch of the collected current, the range of the probe potentials under consideration is limited and sets between the lower value of the polarised potential, which is ~-40 *kT/e,* and the floating potential φ_f , which is ~ -6 *kT/e* for the O+ plasma (see Fig. 6). Therefore, in the considered range the attracted probe energy is higher than proton energy and has the same order of magnitude as the kinetic energy of the oxygen. This is why the highest density of the positive charge in the wake region is expected to be found in the vicinity of the probe. In the Fig.7 density distribution of the electrons (red line) and ions (blue line) along the probe axis parallel to the bulk velocity are presented in the case of the φ=–20 kT/e for (a) the H^+ plasma with V_0 =V_{Tp} and (b) the O^+ plasma with V_0 =4V_{TO}. Plasma parameters are chosen the same as in the Fig. 1. Charge densities are normalised to their values in the non-disturbed

plasma and averaged over the time period $5\omega_{pe}^{-1}$. It worth to note that in the O^+ plasma the region of the charge separation in the wake is increased twice with respect to the H^+ plasma.

Charge anisotropy in the sheath leads to the current anisotropy on the probe surface. In the Fig. 8 the current distributions versus angle between the bulk velocity vector and the external normal to the probe surface are shown for three cases, i.e. $V_0 = V_{Tp}$ (in blue) , $V_0 = 2V_{Tp}$ (in green) in the H^+ plasma and $V_0 = 4V_{To}$ (in red) in the O^+ plasma in the same conditions as in the Fig.7. Dots stand for the numerical solutions and lines for their fit by exponential law. Current is normalized to its value at the angle 0°. The presented solutions demonstrate that current distribution versus angle is almost uniformly distributed on the upstream part of the probe (similar to the case of non flowing plasma), contrary to the distribution on the downstream side which adequately reacts on the wake overloading with the positive charge. Wake side distribution is narrower in the plasma with higher bulk speed or lower ion thermal velocity. This feature together with the ratio of the currents measured at 0° and 180° can provide a tool to deduce the bulk velocity in the ionospheric plasma. Here again we have to mention that photoelectron emission will add an additional asymmetry and in such case the interpretation of the current angular measurements might be problematical.

Conclusions

We propose numerical model of the PIC type which allows to solve the problem of the current collection on the surface of segmented probe. This model was applied for the case of bulk thermal plasma with the characteristics that are expected to be observed in the ionosphere at the altitude of ~700 km. We conclude that currents, which are simultaneously measured by the spherical probe and its segments, might provide a possibility to resolve the flow velocity. To use this model for the interpretation of the Langmuir probe measurements in the ionosphere two additional effects have to be considered, i.e. magnetic field and sun ultra-violet radiation. Each effect will introduce its own asymmetry in the system probe-sheath. First effect will modify the electron branch and second the ion branch of the collected current. These topics will be considered in the following papers.

Acknowledgements

This work was supported by DEMETER/CNES and ESTEC/ESA contracts.

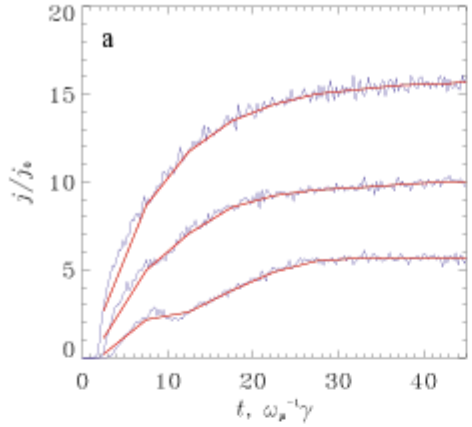

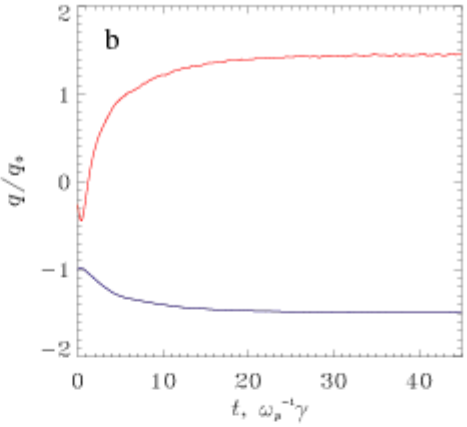

Fig. 1

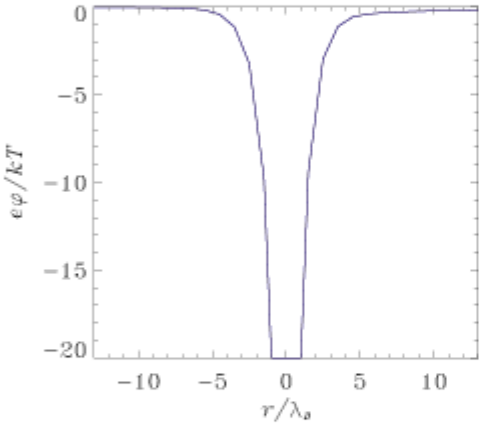

Fig. 2

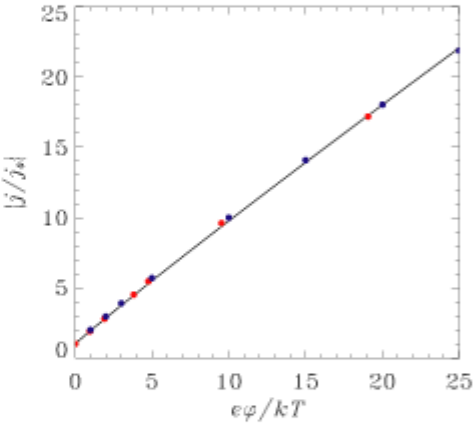

Fig. 3

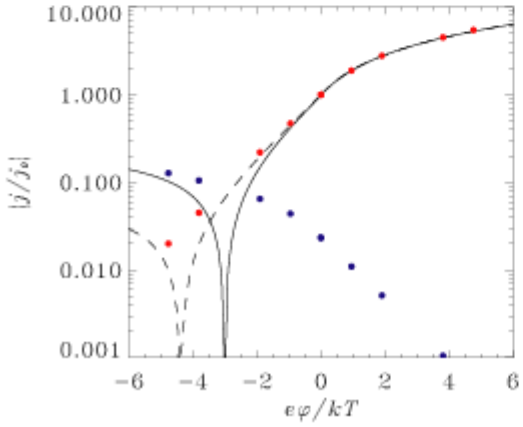

Fig. 4

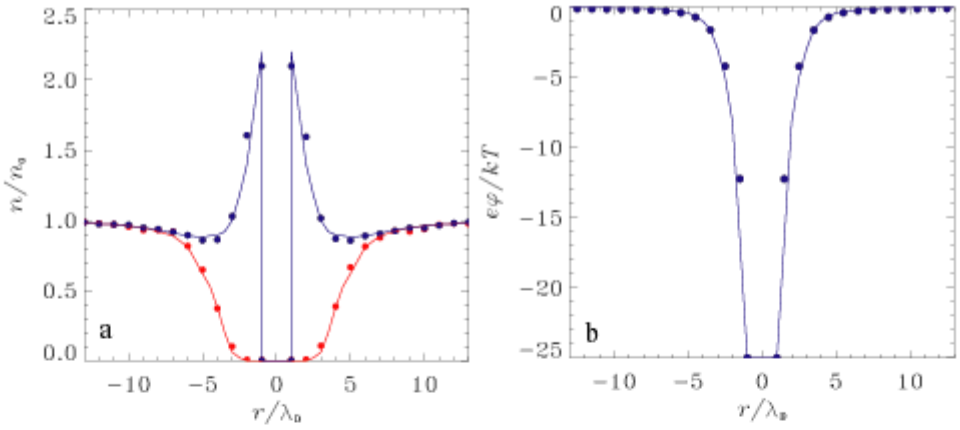

Fig. 5

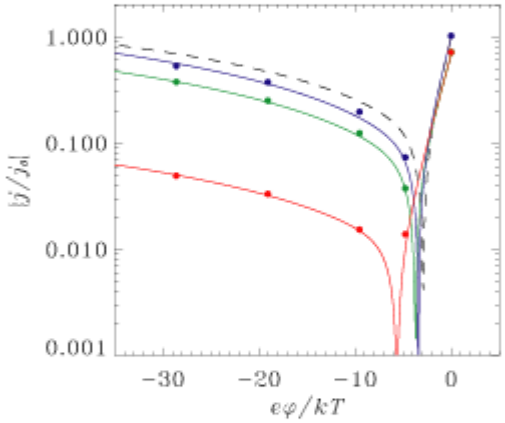

Fig. 6

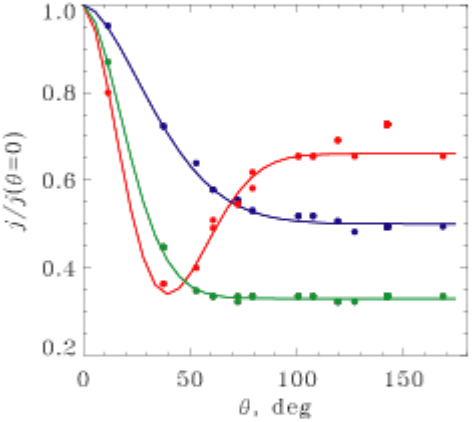

Fig. 8

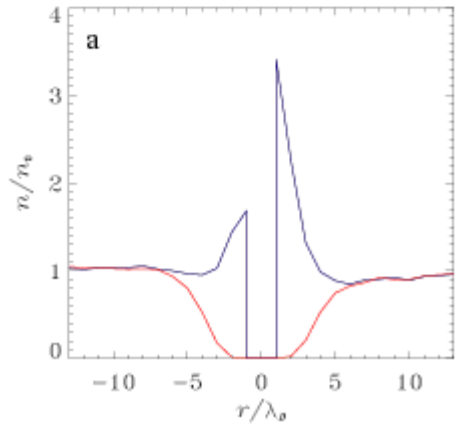

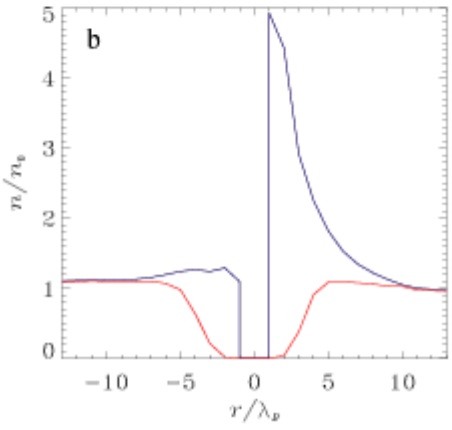

Fig. 7

Figures captures

Figure 1. (a): total current collected by spherical probe in the case φ=–20 kT/e, λ_D=2cm, T = 0.2eV. Upper, middle and lower curves correspond to the H^+ plasma with $V_0 = V_{Tp}$, $V_0 = 2V_{Tp}$ and the O^+ plasma with $V_0 = 4V_{TO}$, respectively. Blue lines represent calculated values of the ion current and red lines stand for their averaging over the period $5\omega_{pe}^{-1}\gamma$. (b): variation of the total space (red line) and surface (blue line) charges for the case $V_0 = V_{Tp}$. Charges are normalised by the surface charge in the vacuum.

Figure 2. Potential distribution along the probe axis parallel to the bulk velocity in the H^+ plasma with $V_0 = V_{Tp}$. Plasma parameters and probe potential are the same as in the Fig.1, potential is normalised by the plasma temperature.

Figure 3. Normalised current as a function of the normalised attractive potential of the spherical probe of radius 2cm in the non-flowing plasma with λ_D=2cm and T_e=T_p=0.2eV. Blue dots show the exact solution of Laframboise, red dots represent the numerical solution, solid line stands for the fitting of the analytical solution.

Figure 4. Normalised current as a function of the normalised potential (attractive and repelling) of the spherical probe in the same plasma conditions as in the Fig. 3. Red and blue points represent the numerical solution for electron and proton currents, respectively, and solid line stands for the total current. Dashed line represents the collected current in the case of the O^+ plasma.

Figure 5. (a) Density distribution for attracted (blue) and repelling (red) particles, (b) the potential profile in the sheath in the case of non-flowing plasma with λ_D=r_s =2cm, probe potential is fixed at φ =–25 kT/e. Analytical solution is shown by the solid lines and model results by dots.

Figure 6. Normalised current versus normalised potential in the H^+ plasma with V_0=0 (black), V_0=V_{Tp} (blue), V_0=$2V_{Tp}$ (green) and in the O^+ plasma with V_0= $4V_{TO}$. Dots indicate computed values, solid lines stand for their fittings. Plasma characteristics are chosen the same as in the Fig. 1.

Figure 7. Positive (in blue) and negative (in red) charge density along the probe axis parallel to the bulk velocity (a) in the H^+ plasma with $V_0 = V_{Tp}$ and (b) in the O^+ plasma with $V_0 = 4V_{TO}$. Plasma parameters and probe potential are the same as in the Fig.1. Charges are normalised by their values in the non-disturbed plasma, distance is normalized by the Debye length.

Figure 8. Current distribution as a function of angle between the vector of plasma bulk velocity and the external normal to the probe surface in the H^+ plasma with V_0=V_{Tp} (in blue), V_0=$2V_{Tp}$ (in green) and in the O^+ plasma with V_0= $4V_{TO}$ (in red). Dots indicate computed values, lines stand for their fits. Plasma characteristics are chosen the same as in the Fig. 1. Current is normalized to its value at the angle 0°.

References

1. Al'pert Ya. L., Waves and artificial bodies in near-Earth plasma, in Russian, Nauka, Moscow, 1974.

2. Béghin, C. and E. Kolesnikova, The Surface-Charge Distribution approach for modellization of quasistatic electric antennas in isotropic thermal plasma, Radio Sci., 33, 503, 1998.

3. Jolivet L. and J. F. Roussel, Numerical simulation of plasma sheath phenomenon in the presence of secondary electronic emission, submitted to IEEE Trans. Plasma Sci., 2001.

4. Hanson, W. B., S. Sanatani, D. Zuccaro, T. W. Flowerday, Plasma measurements with the retarding potential analyser on OGO 6, J. Geophys. Res., 75, 5483-5501, 1970.

5. Kolesnikova, E., Méthode des distributions superficielles de charges pour la modélisation des antennes électriques en plasma homogène, isotrope et Maxwellien, Thèse de Doctorat, Univ. Orléans, 1997.

6. Laframboise, J. G., Theory of spherical and cylindrical Langmuir probes in a collisionless, Maxwellian plasma at rest, UTIAS report N 100, Institute for aerospace studies, University of Toronto, 1966.

7. Laframboise, J. G. and L. J. Sonmor, Current collection by probes and electrodes in space magnetoplasma : a reveiw, J. Geophys. Res., 98, 337-357, 1993.

8. Lebreton, J.-P., Micro-satellite DEMETER, DCI-ISL, Technical note, ESTEC SCI-SO, 2002.

9. Roussel, J. F. and J. J. Berthelier, A study of the electrical charging of the ROSETA Orbiter, I-Numerical Model, J. Geophys. Res.-Planets, accepted for publication, 2003.

10. Sanmartin, J. R., Theory of a probe in a strong magnetic field, Phys. Fluids, 13, 1970.

11. Séran, E., Reconstruction of the ion plasma parameters from the current measurements: Mathematical tool, Annales Geophysicae, 21, 1159-1166, 2003.